Scaling Behavior in Quasi Static and Impact Fragmentation of Brittle Materials

Marina Davydova[1,*], Sergey Uvarov[1]

[1] Institute of Continuous Media Mechanics, Ural Branch of Russian Academy of Sciences, Perm 614013, Russia
* Corresponding author: davydova@icmm.ru

Abstract An investigation was conducted to examine experimentally the process of fragmentation of brittle materials (glass plates and quartz rods) under quasi-static and dynamic loading conditions. In the quasi-static tests of glass plates, two types of scaling laws were considered. Of these, one was based on the fractal relation similar to the Dielectric Breakdown Model or the Diffusion-limited Aggregation Model, and the other involved the definition of the fragment size distribution. The results of investigation indicate that fragment size distributions mainly follow power-law distributions. Variations in the fragmentation mechanism correlate with quantitative changes in the fractal dimension observed in different regions of the fragmented specimen. The dynamic fragmentation statistics was studied in the recovery experiments with quartz cylindrical rods. The mechanoluminescence-based method was used to measure the distribution of time quantities. Impact loading applied to specimens leads to the formation of fracture surfaces, which produces intensive light emission registered then by Photo Multiplayer Tubes. The data recovery technique allows us to save the fragments and to determine the size distribution of fragments. Both the fragment size distribution and the time interval distribution show evidence of obeying scaling laws.

Keywords: Fractal, Brittle fragmentation, Scaling law, Self-organized criticality

1. Introduction

Results of fragmentation processes (the breakup of matter into smaller pieces) are visible everywhere. In nature these may be rock fragments of sizes varying from stones to sand and dust, or arctic sea ice fragments. Almost all kinds of explosions and collisions result in fragmentation. Common to brittle fragmentation processes is that the fragment-size distribution is given by a power law [1-8]. The origin of this power law has attracted much attention lately. The assumption that the exponential distribution is typical of the fragmentation of ductile materials and the power-law distribution characterizes brittle fragmentation has been discussed by Grady [9]. However, in some experiments with brittle materials the exponential or log-normal laws were observed [10-13]. Donald Turcotte [14] has pursued the fragmentation of brittle materials as a fractal process resulting in the power law distribution function $N \sim x^{-D}$, where N is the number of fragments, x is the linear dimension of fragments, and D is the fractal dimension. The fractal character of the distribution function in a wide range of fragment sizes allows Oddershede et al. [7] to suppose that the fragmentation exhibits self-organized criticality (SOC) [15].

2. Glass fragmentation

Fragmentation processes are complex and involve propagation of many cracks and their interaction. Therefore, it is of interest to study the overall statistical aspects. Quasi-static testing was performed in the experiments with glass plates loaded in a “sandwich” to save the glass fragmentation pictures (Fig. 1a). Using the original software, the images were transformed into the schematic pictures corresponding to the fragmentation patterns (Fig. 1b).

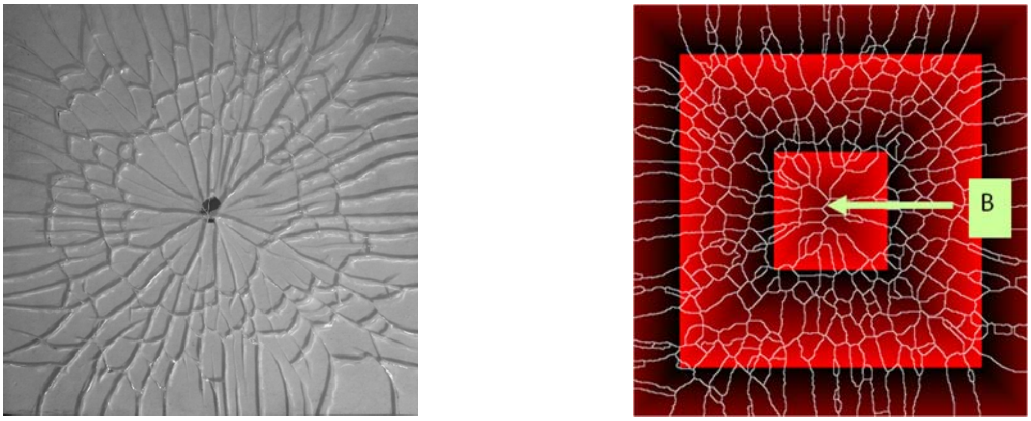

a) b)

Figure 1. a) Photographs of typical fragmentation patterns. b) Schematic pictures of fragmentation patterns to determine the size and number of fragments and the total length of cracks.

This made it possible to determine the size and number of fragments and the total length of cracks. We consider two types of scaling. The first type is based on the relation

$$L(r) \sim r^{D}, \tag{1}$$

where $L(r)$ is the total crack length in the boxes of a size $r \times r$ centred at the point B (Fig. 1b), and D is the fractal dimension. The second type is the traditional definition of the cumulative distribution of fragment sizes, that is, the calculation of the number of fragments N with a size larger than S.

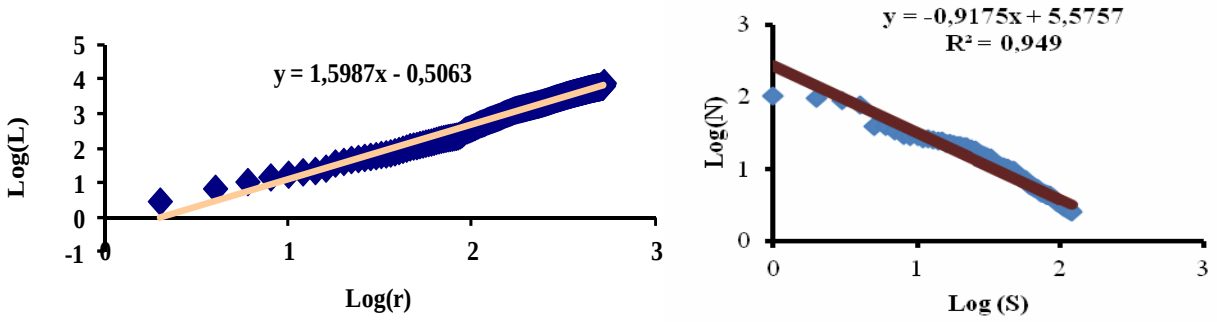

a) b)

Figure 2. a) Scaling law obtained using the relation for crack length (1). b) Cumulative log-log plots of the fragments size distributions.

The use of Eq. (1) was discussed by Sornette et al. [16]. However, it should be noted that the fracture pattern [16] does not have a distinct central point. At the same time, the examined fragmentation patterns have a central point, and their configuration is similar to that created with the

model of diffusion-limited aggregation (DLA) [17] or the model of dielectric breakdown (DB) [18]. Relation (Eq.1) can be used to define the fractal dimension for both these models. In the case of the DB model, $L(r)$ is the total length of the discharge branches within the circle of radius r For the DLA model, $L(r)$ is the number of particles. By analogy with the DLA and DB models, to determine the fractal dimension of the fragmentation patterns, we use Eq.(1), where $L(r)$ is the total length of cracks in the boxes of a size $r \times r$ centred at the point B (Fig. 1b). The minimal number of the boxes used for calculation of the fractal dimension is 200. The scaling law obtained using the relation for crack length (Eq.1) is presented in Fig. 2a. The processing of the fragment sizes shows that the relation between the fragment area and the number is also fitted by a power law (Fig. 2b and Fig. 6).

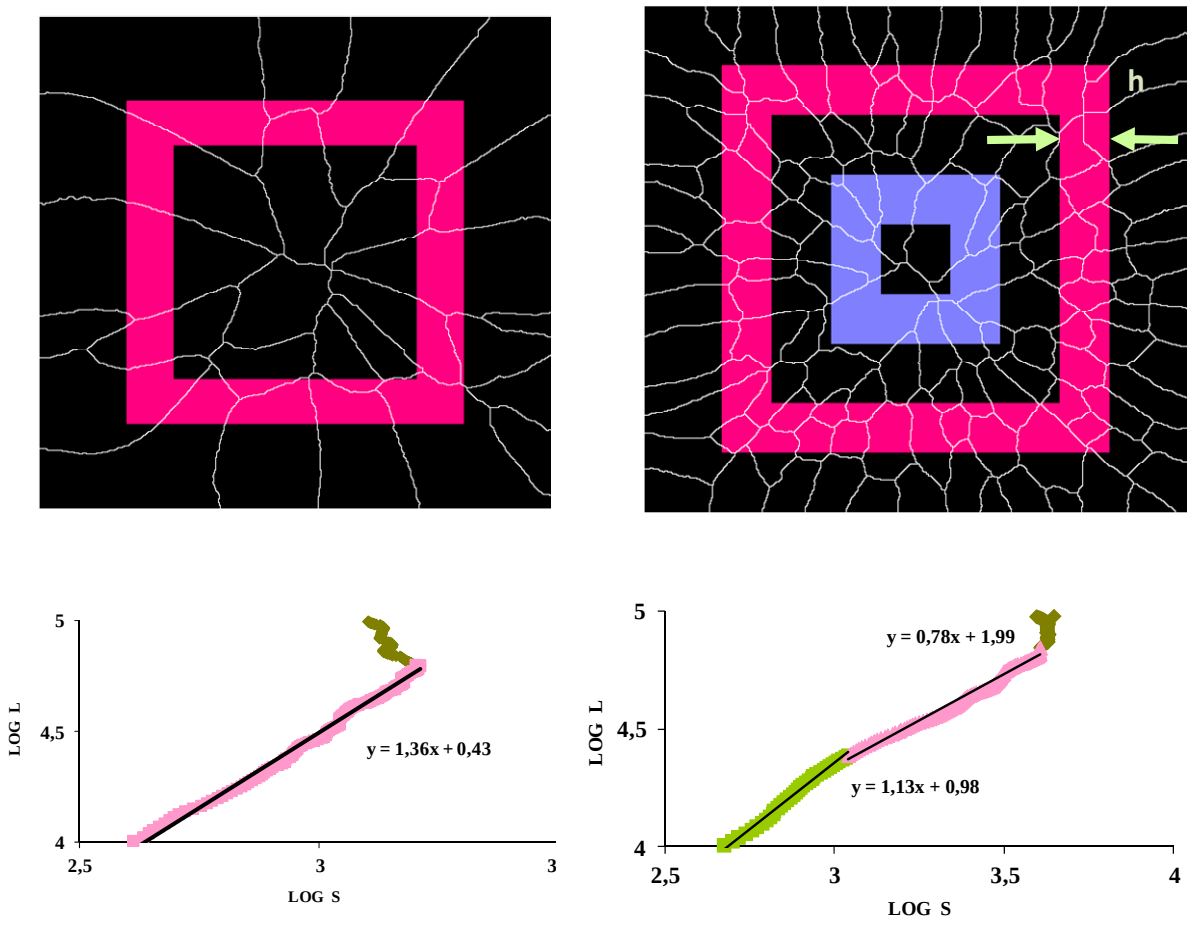

a) b)

Figure 3. a) Fragmentation pattern and fractal dimension definition for the fracture accompanied by radial crack formation. b) Fragmentation pattern and fractal dimension definition for the fracture accompanied by a change in the fracture mechanism.

There are two types of energy-dependent fragmentation patterns leading to a breakup (Fig. 3). Fig.3a presents a fragmentation pattern that illustrates the fracture accompanied by radial crack formation. The right fragmentation pattern (Fig. 3b) has two zones corresponding to two different fracture mechanisms. The central zone has a radial crack only. In the second zone, the crack

branching process is observed. Assuming that different fracture mechanisms characterize different fractal dimensions, we have

$$L(S) \sim S^D, \tag{2}$$

where $L(S)$ is the total crack length inside the square frame with a thickness h (Fig. 3b), S is the frame area, and D is the fractal dimension. Calculation the fractal dimension using expression (Eq.2) shows that, for the left fragmentation pattern (Fig. 3a), the data is fitted by a single line. For the right pattern, the log-log representation of $L(S)$ changes its slope, and the power-law exponent D decreases. A change in the fracture mechanism (from radial crack formation to crack branching) correlates with the qualitative changes in the fractal dimension.

3. Quartz fragmentation

3.1. Loading condition.

The first stage of the experiment was to evaluate the effect of loading conditions and the shape and size of the sample on the fragment size distribution function. Three types of loading conditions (I, II, III) were realized using a ballistic set-up:

- fragmentation as a result of interaction of direct and reflected compression waves (I) (Fig.4a);
- fragmentation under the action of a compression wave (II) (Fig.4b);
- fragmentation induced by a direct compression wave and its reverberation in rod (III) (Fig.4c).

Loading Condition I. The ballistic set-up consists of a gas gun with a bore of 19.3 mm diameter, a velocity registration system, and a base where the sample is mounted (Fig. 4a). The sectional glass rod is composed of a buffer and the main part covered by an elastic shell. The buffer was used for realization of uniaxial loading produced by a cylindrical projectile of mass 13.9 g accelerated up to the velocities of 6-22 m/s.

Loading Condition II. To avoid the possible influence of the reflected wave on the fragmentation scenario, the ballistic set-up was modified. The sample was placed into a steel cylinder filled with plastic foam (Fig. 4b). The sectional glass rod was composed of a buffer, main part and outer parts. The presence of the last part made it possible to catch the reflected wave.

Loading Condition III. The scheme given in Fig. 4c illustrates the experimental technique used to measure the distribution of time quantities. Impact leads to the formation of fracture surfaces, which produce intensive light emission (mechanoluminescence or fractoluminescence).The intensity of the light is registered by the Photo Multiplayer Tube connected with the oscilloscope (oscilloscope sample rate is 1 GHz).

3.2. Fragment mass distribution.

The mass of the fragments passing through the sieves was obtained by weighing the fragments using an electronic balance HR-202i (accuracy 10^{-4} g). The mass of the fragments corresponding to the maximum of the probability density function varied in the range from $2*10^{-4}$g to $6*10^{-4}$ g

(Fig.5a). At low energy, a more considerable scattering was found for this value (Fig.5b). This actually means that for low energy we have two or three sieves with a comparable number of fragments, and for high energy - only one sieve with a predominant number of fragments.

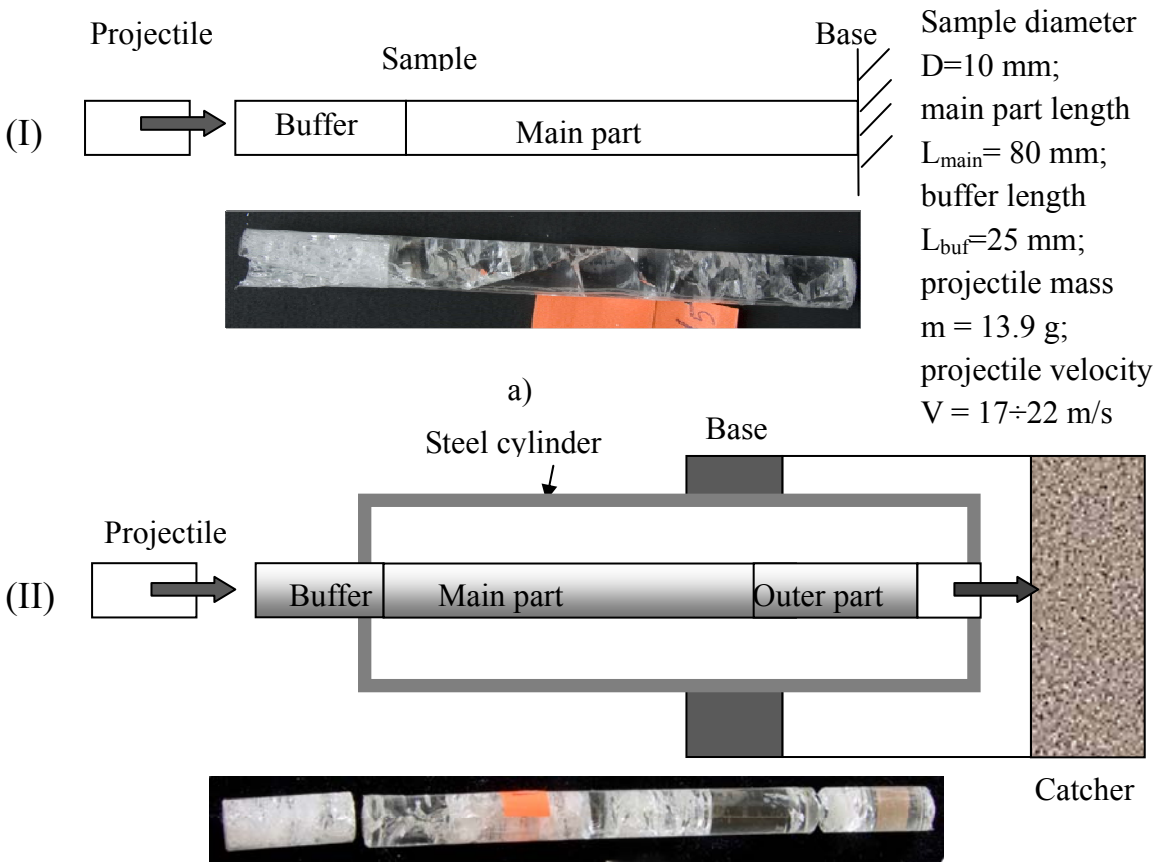

Sample diameter D=12 mm; main part length L_{main} = 120 mm; buffer length L_{buf} =25 mm; outer part length L_{out}= 30 мм; projectile mass m = 6.3 g; V = 40÷50 m/s

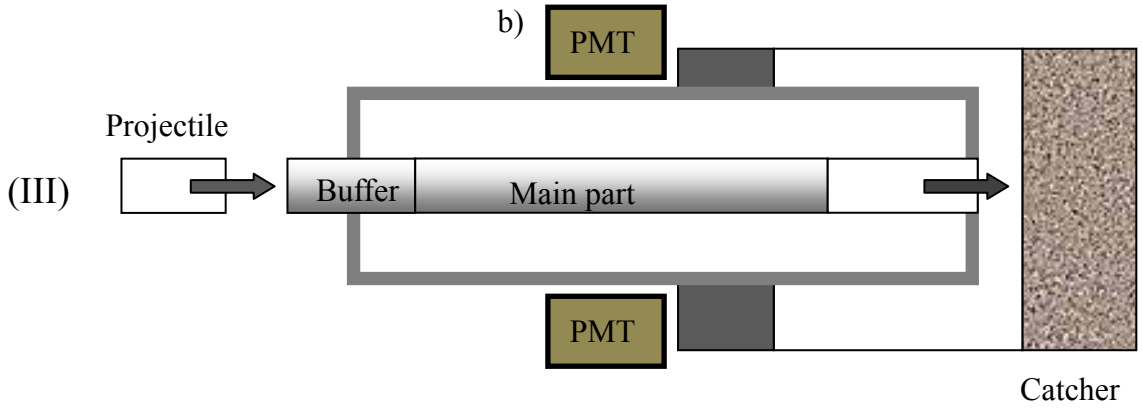

Sample diameter D=12 mm; main part length L_{main} = 120 mm; buffer length L_{buf} =25 мм;

c)

Figure 4. Schemes of loading: a) condition I; b) condition II; c) condition III.

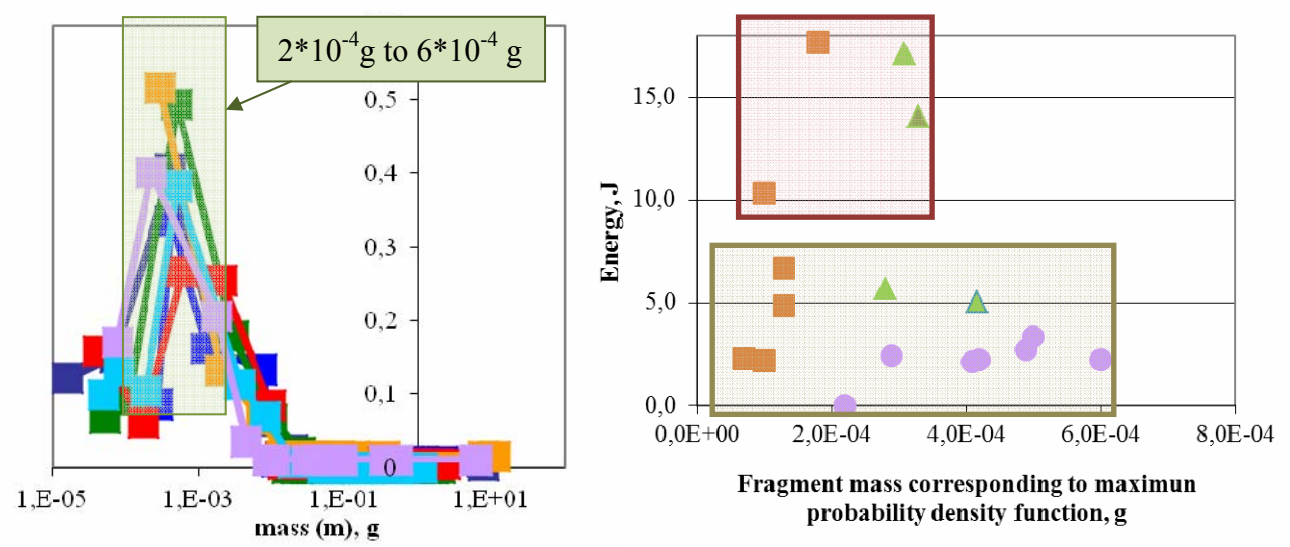

a) b)

Figure 5. a) Probability density function. b) Dependence of the fragment mass corresponding to maximum probability density function on the projectile energy. The markers indicate the loading type: I-circles; II-triangles; III-boxes.

The fragmentation statistics was analyzed by varying the sample size and load intensity (projectile velocity). The results of experiments have indicated that the variation in the sample size and loading conditions does not lead to the change in the type of the probability density function.

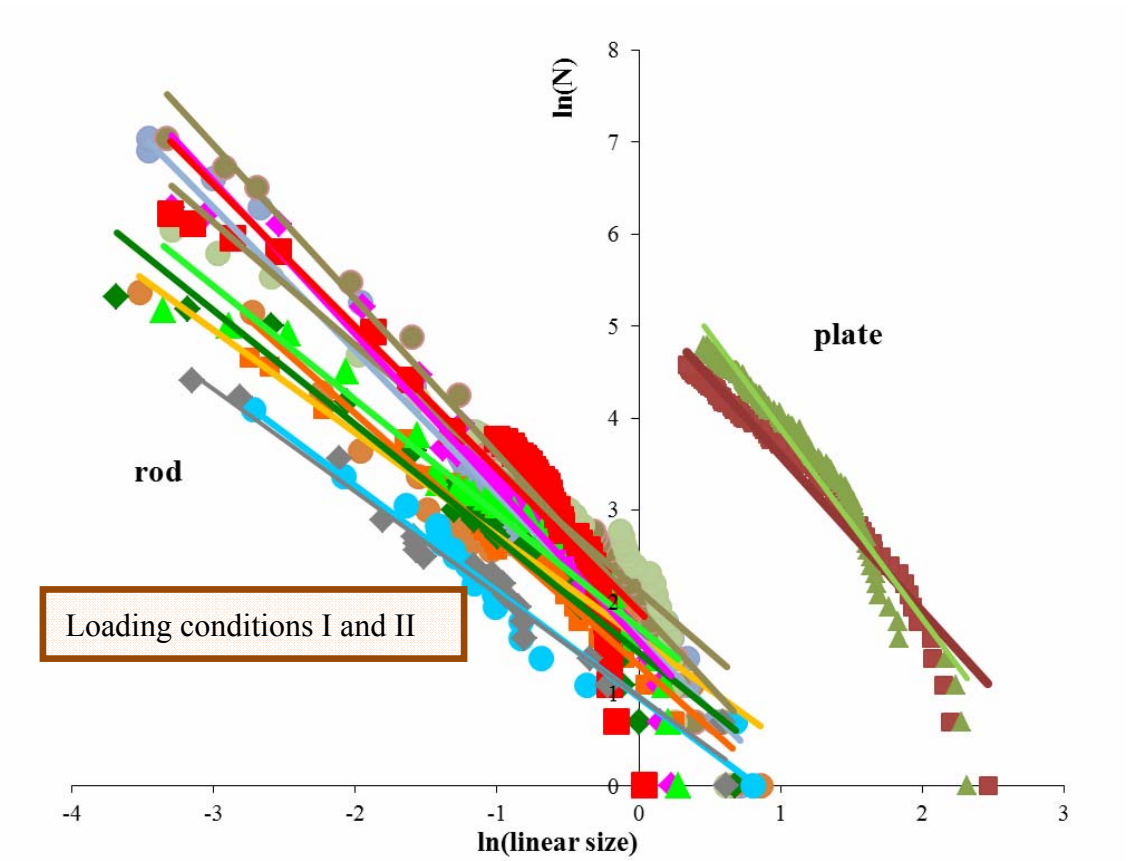

Figure 6. Double logarithmic plot of the cumulative distribution function for plate and rod.

Thus, the cumulative distributions illustrating the relation between the numbers of fragments and their linear dimension are represented as a log-log plot (Fig. 6). The linear dimension is defined as a cube root of mass or a square root of area. The distribution is fractal by nature with a power law in the form $N(>r) = Cr^{-D}$, where N is the number of fragments with a characteristic linear dimension greater than r. The fractal dimension D varies from 1.6 to 2.0 for the plate and from 1.1 to 1.7 for the rod (Loading Conditions I and II).

3.3 Distribution of time interval between the impulses of intensive light emission

To measure the scaling of spatial and time quantities corresponding to the same sample, we have developed the experimental scheme presented in Fig.4c (Loading Condition III). Fracture surfaces formed under impact loading produced intensive light emission (mechanoluminescence or fractoluminescence). The mechanoluminescence impulses were registered by two PMT connected with the oscilloscope (Fig.7). The second PMT was used to provide the reliability of measurements.

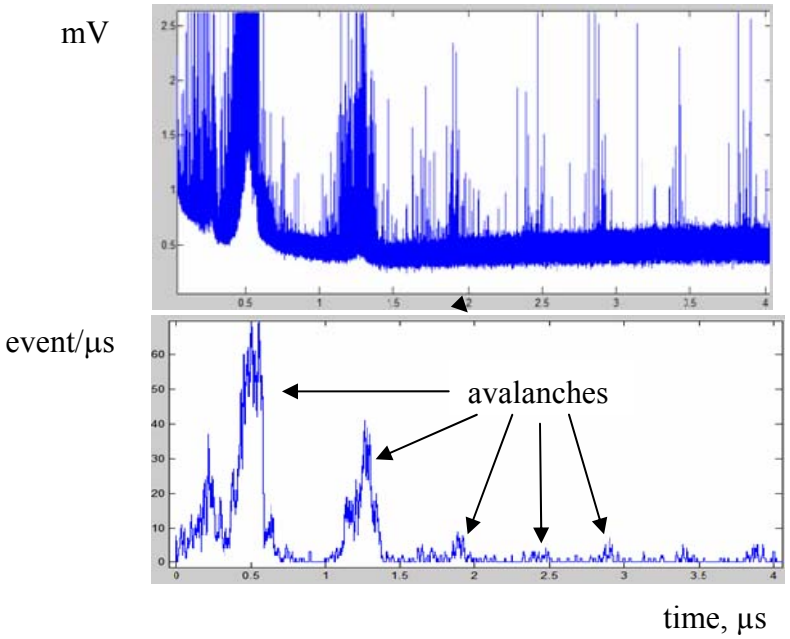

Figure. 7. Signal of the oscilloscope and the frequency of impulse appearance.

The process of light reflection looks like the process of avalanche spreading (Fig. 7). The lower plot represents the event frequency. The events are distributed in blocks.

The cumulative distribution function of the time interval (registered by two PMT) in the double logarithmic plot (Fig.8b) is fitted by the straight line (90% of the total number points). At small sizes (8% of the total number of points), the curve deviates from the straight line because the size of time interval is comparable with the oscilloscope sample rate (1 GHz). The falloff at the largest interval sizes (2% of the total number of points) is due to finite-size effects. In this case, the time interval is comparable with the process time. The central part is the line covering 90% of the total number of points. It has been found that the fragment size distributions (Fig.8a) and the time interval

distributions (Fig.8b) obey scaling laws, which suggests the possibility of self-organized criticality in fragmentation.

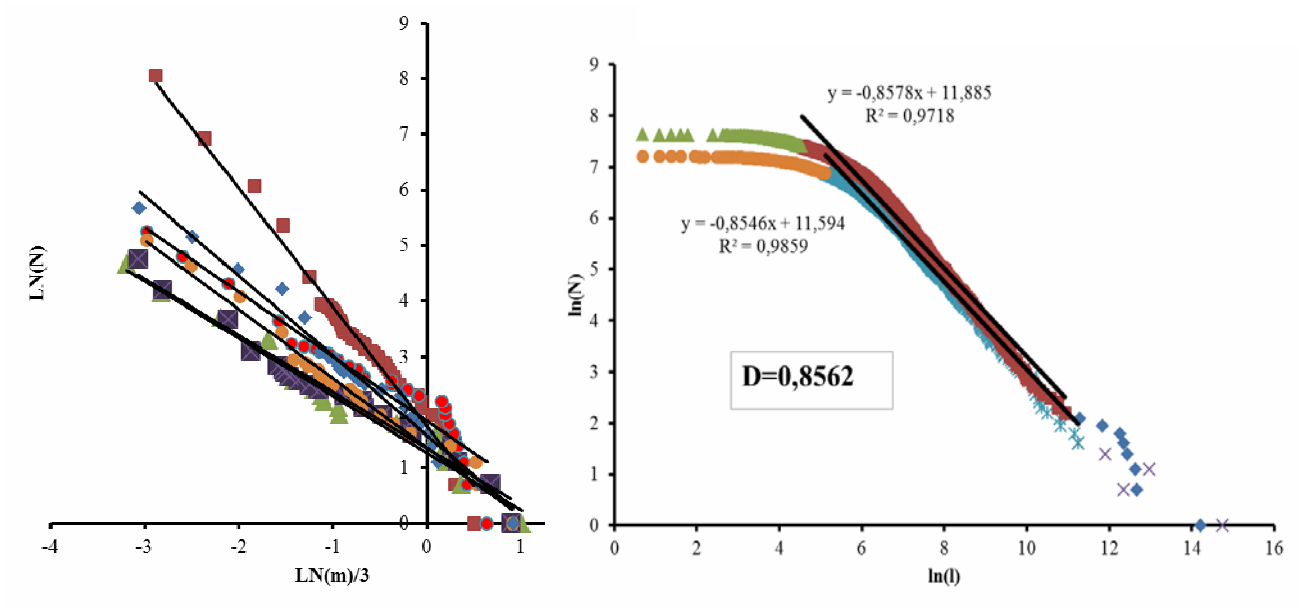

a) b)

Figure 8. a) Fragment size distribution (spatial scaling) for loading condition III. b) Distribution of time interval separating the fractoluminescence impulses (for one sample). *D* is the average exponent for the signals corresponding to two PMT placed near the opposite side of the sample.

The fractal dimension D varies from 1.02 to 2.14 for the spatial variable (Fig.8) and from 0.28 to 0.85 for the time variable (Fig.9).

4. Conclusion

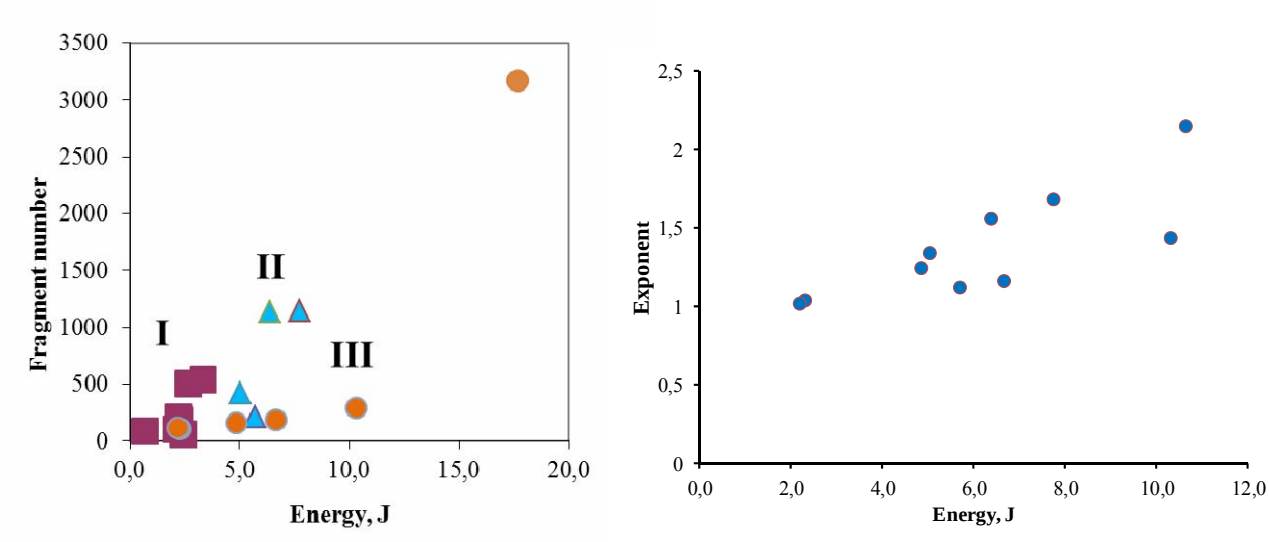

a) b)

Figure 9. a) Fragment number versus projectile energy. I, II, III indicate loading conditions. b) Power law exponent for different levels of projectile energy.

Experimental investigations were carried out to examine the fragmentation of brittle materials under quasi-static and dynamic loading conditions. Based on the obtained results, the following conclusions can be derived:

- fragmentation patterns of glass plates are fractal;
- variation in the fracture mechanism of plates correlates with the changes in the fractal dimension;
- number of fragments occurred during the fragmentation of quartz rods (Fig. 9a) depends on loading conditions;
- power law exponent for fragment size distributions of quartz (Fig. 9b) increases with growth of projectile energy;
- fragment size distribution for the observed type of fragmentation (glass plates and quartz rods) is fractal and satisfies the relation $N(>r) = Cr^{-D}$;
- fragment size distributions and time interval distributions are governed by scaling laws, which is indicative of the self-organized critical behavior during the fragmentation process.

Acknowledgements

The author would like to acknowledge the Russian Foundation for Basic Research (grant RFBR 11-01-96010, grant RFBR 11-01-00712)

References

[1] R.Ye. Brodskii, P.V. Konevskiy, R.I. Safronov, Size distribution of sapphire fragments in shock fragmentation. Functional Materials, 18, N2 (2011) 200-205.

[2] E.S.C. Ching, S.L. Lui, Ke-Qing Xia, Energy dependence of impact fragmentation of long glass rods. Physica A, 287 (2000) 83 – 90.

[3] T. Kadono, Fragment mass distribution of plate like objects. Physical Review Letters, 78, N 8, (1997) 1444-1447.

[4] T. Kadono, M. Arakawa, Crack propagation in thin glass plates caused by high velocity impact. Physical Review E, 65, (2002) 035107(R)

[5] H. Katsuragi, D. Sugino, H. Honjo, Scaling of impact fragmentation near the critical point. Physical Review E 68, (2003) 046105

[6] A. Meibom, I. Balslev, Composite Power Laws in Shock Fragmentation. Physical Review Letters, 76, N14 (1996) 2492-2494.

[7] L. Oddershede, P. Dimon, J. Bohr, Self-organized criticality in fragmenting. Physical Review Letters, 71, N 19 (1993) 3107-3110.

[8] F. P. M. dos Santos, V. C. Barbosa, R. Donangelo, S. R. Souza, Experimental analysis of lateral impact on planar brittle material. Physical Review E 81, (2010) 046108

[9] D.E. Grady, Length scales and size distributions in dynamic fragmentation. International Journal of Fracture, 153, N 1-2 (2010), 85-99.

[10] J. A. Astrom, R. P. Linna, J. Timonen, P. F. Moller, L. Oddershede, Exponential and power-law mass distributions in brittle fragmentation. Physical Review E 70, (2004) 026104

[11] H. Katsuragi, S. Ihara, H. Honjo, Explosive fragmentation of a thin ceramic tube using pulsed power. Physical Review Letters, 95, (2005) 095503

[12] H. Katsuragi, D. Sugino, H. Honjo, Crossover of weighted mean fragment mass scaling in two-dimensional brittle fragmentation. Physical Review E 70, (2004) 065103(R)

[13] V.V. Sil'vestrov, Application of the gilvarry distribution to the statistical description of fragmentation of solids under dynamic loading. Combustion, Explosion, and Shock Waves, 40, N 2, (2004) 225–237.

[14] D. L.Turcotte, Fractals and chaos in geology and geophysics, Cambridge University Press, UK, 1997.

[15] P.Bak, C.Tang, K.Wiesenfeld, Self-organized criticality: an explanation of 1/f noise. Physical Review Letters, 59, N4 (1987) 381-384.

[16] A.Sornette, P. Davy, D.Sornette, Growth of fractal fault patterns. Physical Review Letters, 65, N18 (1990) 2266-2269.

[17] L.Niemeyer, L.Pietronero, and H.J.Wiesmann, Fractal Dimension of Dielectric Breakdown. Vol. Physical Review Letters, 52, N12, (1984) 1033-1036.

[18] T.A.Witten, L.M.Sander, Diffusion-limited aggregation, a kinetic critical phenomenon. Physical Review Letters 47, N19 (1981) 1400-1403.